Dual Pore Network Model of Electrical Resistivity for Carbonate Rocks

D. Ahmadi, M. Ioannidis

Department of Chemical Engineering, University of Waterloo, Canada

This paper was prepared for presentation at the International Symposium of the Society of Core Analysts held in Avignon, France, 8-11 September, 2014

ABSTRACT

We develop a model which explains the non-Archie behavior of carbonate rocks with multi-scale structure. Non-Archie behavior in such rocks is qualitatively related to the degree of connectedness (percolation) of different water fractions, namely water residing in networks comprising pores of very disparate scales (micro-porosity and macro-porosity). To this end, we investigate here a previously reported dual pore network model (D-PNM) which allows for heterogeneous matrix (micro-porosity) properties and variably-connected macro-porosity. By varying the relative amounts, geometric properties and degree of connectedness of micro-porosity and macro-porosity, we are able to stylistically reproduce all documented deviations of the resistivity index from Archie behavior.

INTRODUCTION

Interpretation of measured electrical resistivity of reservoir rocks, needed for estimating the hydrocarbon content, is traditionally based on Archie's original equations, which often are employed assuming cementation and saturation exponents equal to 2. Carbonate rocks, however, exhibit significant deviations from Archie's relations: the cementation exponent may vary widely (from 1.45 to 5.4) [1] and the resistivity index curve may demonstrate nonlinear trend on a log-log scale [2]. This behavior is understood to originate from the existence within carbonate rocks of at least two different pore systems, but is not fully quantified. Petricola and Watfa considered dual pore geometry to highlight the significant influence of microporosity on electrical resistivity and the estimation of water saturation thereof [4]. Using effective medium theory to compute the effect of microporosity on resistivity, Sen has pointed out the anomalously large resistivity increase as the conducting water phase becomes trapped in isolated regions [5], whereas Dixon and Marek suggested that a network of interconnected micropores may explain anomalously low saturation exponents [3]. Han et al. [6] further proposed that for carbonate samples with a double pore size distribution, the electrical behavior should depend strongly on the spatial distribution and connectivity of the micro-porosity. Recently, Bauer et al. reproduced electrical responses of two different carbonates using a D-PNM parameterized on the basis of extensive analysis of high-resolution micro-tomographic data [7]. Their work, which to our knowledge represents the most sophisticated attempt to quantify the electrical resistivity behavior of carbonates, drew attention to significant uncertainty owed to the inability of currently available methods to resolve all length scales of relevance to current transport.

Our model of the electrical resistivity of dual pore systems is based on the original work of Ioannidis and Chatzis [8]. We show that the D-PNM can reproduce the behavior of electrical resistivity for two different types of carbonates discussed in the recent literature [7] while being

consistent with capillary pressure data. Parametric studies further confirm the model's ability to stylistically reproduce all documented deviations of the resistivity index from Archie behavior [2], suggesting opportunities for rapid assessment via a constrained optimization approach conditioned on microtomographic data.

METHODOLOGY

The dual pore network (D-PNM) model corresponds to a tessellation of the bulk rock space in cubic cells of side length ℓ (Figure 1a). Each cell comprises *geometrically unresolved* pore space (hereafter referred to as matrix) of known macroscopic properties (porosity, permeability, capillary pressure, cementation and saturation exponents) and *geometrically resolved* secondary porosity in the form of a cubic vug (side length a) at the cell's center connected to six channels of rectangular cross-section (side length b, where R = b/a). The vug size is determined from knowledge of the cell size ℓ and local vug porosity [8]. Although the latter is here assumed to follow a Weibull distribution, it may be calibrated to local porosity measurements obtained by x-ray microtomography. The connectivity of the secondary pore space can be adjusted to yield models with varying degrees of percolation of the secondary porosity. Matrix properties may also be spatially distributed and percolation of the matrix pore space may be adjusted by designating a fraction (f_m^o) of cells with negligible matrix porosity. Figure 1b-d schematically depicts D-PNM in which either one or both of matrix and secondary pore spaces form percolating networks.

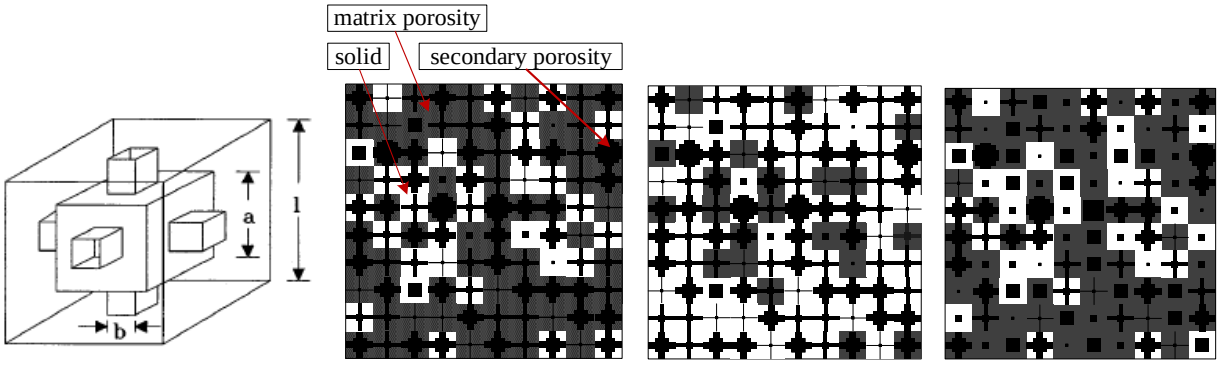

Figure 1. (a) Geometry of a single cell within D-PNM depicting secondary porosity in a background of matrix [8]; Cartoon representation of D-PNM with 10x10 cells; (b) Percolating vugs in percolating matrix; (c) Percolating vugs in non-percolating matrix; (d) Non-percolating vugs in percolating matrix.

Communication between two neighboring cells through secondary pore space (vugs) is controlled by the amount of secondary porosity in adjacent cells and a connectivity exponent ω, as described in [8]. Cells may be invaded by a non-wetting phase via matrix or secondary pore space according to the rules governing capillarity-dominated (quasi-static) displacement and a cluster multiple labeling algorithm is employed to determine the occupancy of matrix and secondary porosity in each cell. This enables the determination of water saturation as a function of increasing capillary pressure (drainage simulation). The electrical resistivity of each cell, which is isotropic, is then determined by assuming conduction through matrix in parallel with conduction through secondary pores, as explained in Eq. 1 and Eq. 2 and Figure 2a-b. In these

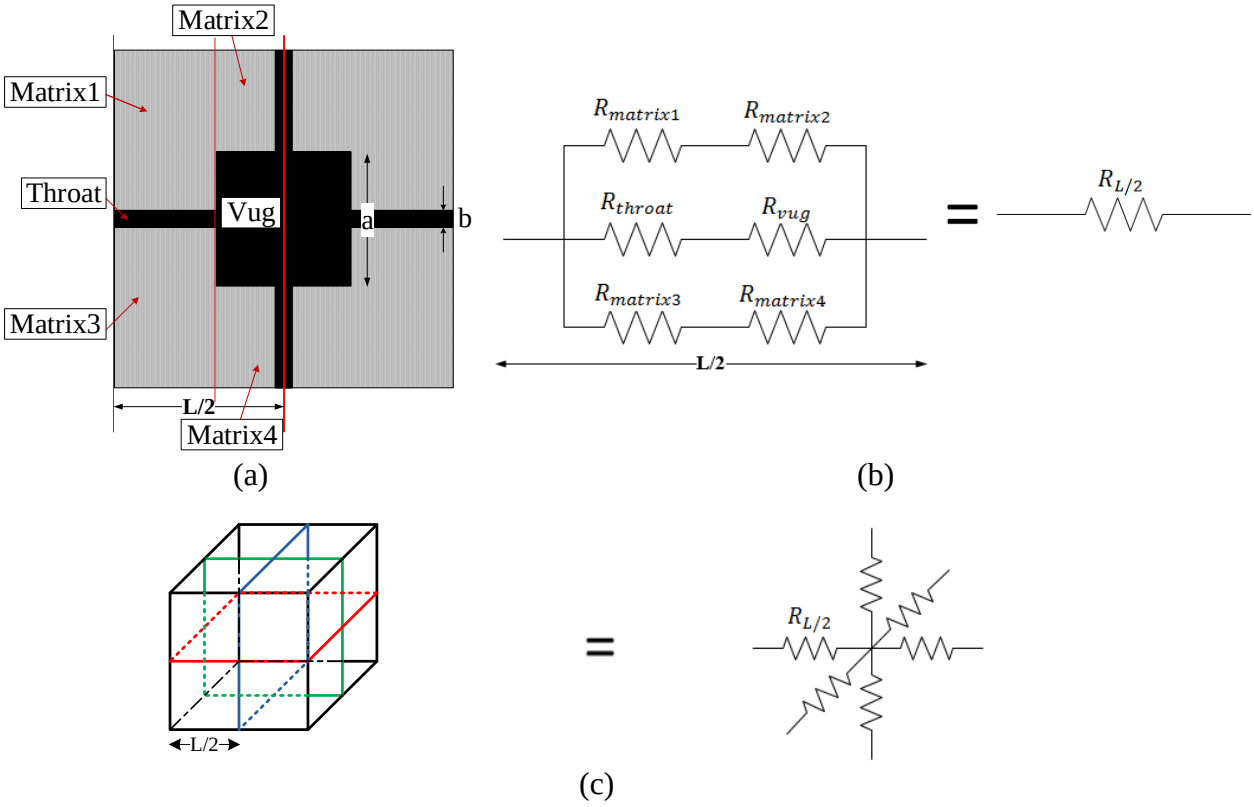

Figure 2. (a) Half-cell resistivity along one direction considering (b) conduction through matrix in parallel with conduction through secondary pores; (c) Single cell represented in 3D by six identical resistors.

$$R_{L/2} = R_{matrix} || (R_{throat} + R_{vug}) \quad (1)$$

$$1/R_{L/2} = 1/R_{matrix} + 1/(R_{throat} + R_{vug}) \quad (2)$$

equations, R_{matrix}, R_{throat} and R_{vug} are all functions of water saturation. Archie's law with known m and n is used to determine R_{matrix}, whereas R_{throat} and R_{vug} are computed as described elsewhere [9]. The resistivity of each cell within the D-PNM is modeled by two half-cells along each orthogonal direction, as shown in Figure 2c. The electrical resistivity of the entire D-PNM is determined by a renormalization approach [10,11]. All results shown here are from D-PNM of size 32x32x32.

RESULTS AND CONCLUSION

The electrical and capillary response of a single cell (φ_{total}= 0.2) for two sets of parameters, referred to as CELL1 (φ_{matrix}= 0.05, R = 0.1) and CELL2 (φ_{matrix}= 0, R = 0.03), are shown in Figure 3, which portrays deviation from Archie's law as inherent to the existence of porosity at two different scales. D-PNM fits to electrical resistivity and capillary pressure data for the Estaillades and Lavoux carbonate samples are shown in Figure 4 and Figure 5, respectively. Using the parameters listed in Table 1, the D-PNM also reproduces the formation factor of both samples (see Table 2), while being consistent with the pore size distributions determined by

mercury porosimetry. The Estaillades sample is represented by a percolating secondary pore space network superimposed on non-percolating matrix (Figure 1c), whereas the Lavoux sample is represented by matrix and secondary pore space networks which are both percolating (Figure 1b). These results are consistent with those of Bauer et al. [8]. In the context of the D-PNM, the curving upwards of the resistivity index at $S_w \approx 0.4$ for the Estaillades sample is associated with the rapid loss of the conductivity of water remaining in nwp-invaded secondary pores as the capillary pressure is increased. This effect is manifested when the matrix porosity is non-percolating. In the case of percolating matrix (Figure 5a), conduction through the matrix pores causes a leveling off of the resistivity index at lower saturations.

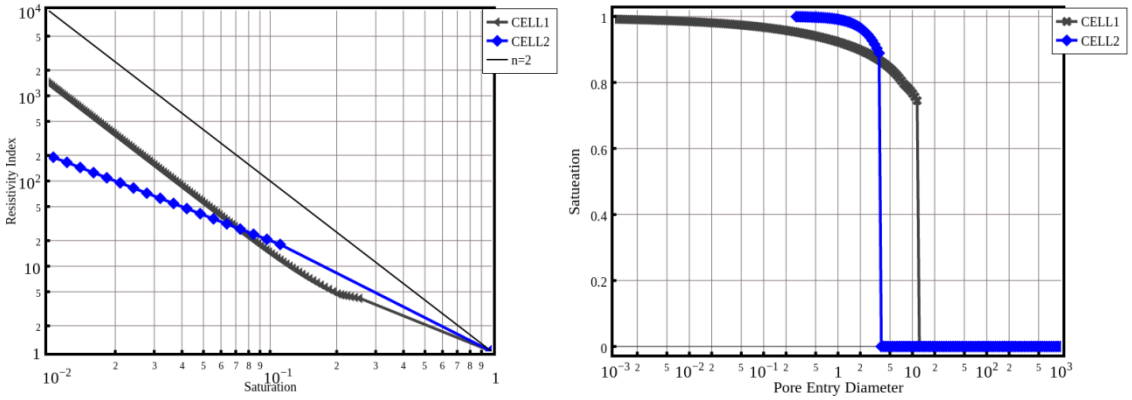

Figure 3. Single cell model response: (left) resistivity index vs. saturation, (right) pore entry diameter distribution.

Table 1. DPNM parameters

Sample	ϕ_{vug}	ϕ_{matrix}	R	ω	f_m°	ℓ (µm)
Estaillades	15	30	0.25	0.815	0.7	200
Lavoux	12.65	28	0.4	0.8	0.4	200

Table 2. Porosity and formation factor of real samples and DPNM

Sample	ϕ_{total}^{Exp} (%)	ϕ_{total}^{DPNM} (%)	FF^{Exp}	FF^{DPNM}
Estaillades	24.7	23.9	24	27.3
Lavoux	28.7	28.5	13	13.7

Finally, Figure 6 demonstrates significant sensitivity of resistivity index prediction for drainage in the Estaillades sample to variations in D-PNM model parameters f_m^o, R, ω and shape of the Weibull distribution. The D-PNM is therefore seen to be able to reproduce different types of nonlinear saturation-resistivity index trends [2] using physically meaningful parameters. It could be used in inverse modeling mode to assert models of dual porosity carbonates consistent with petrophysical and petrographic data in a cost-effective manner.

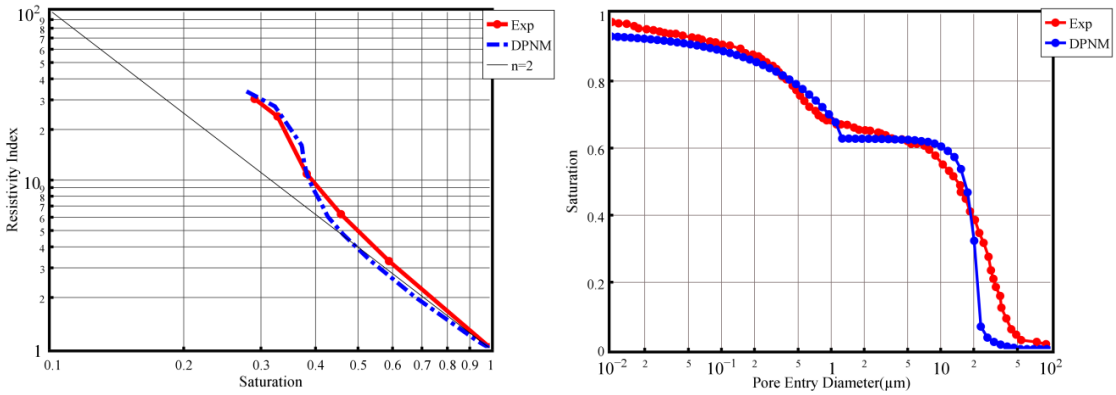

Figure 4. Estaillades carbonate sample: (left) resistivity index vs. saturation, (right) pore entry diameter distribution.

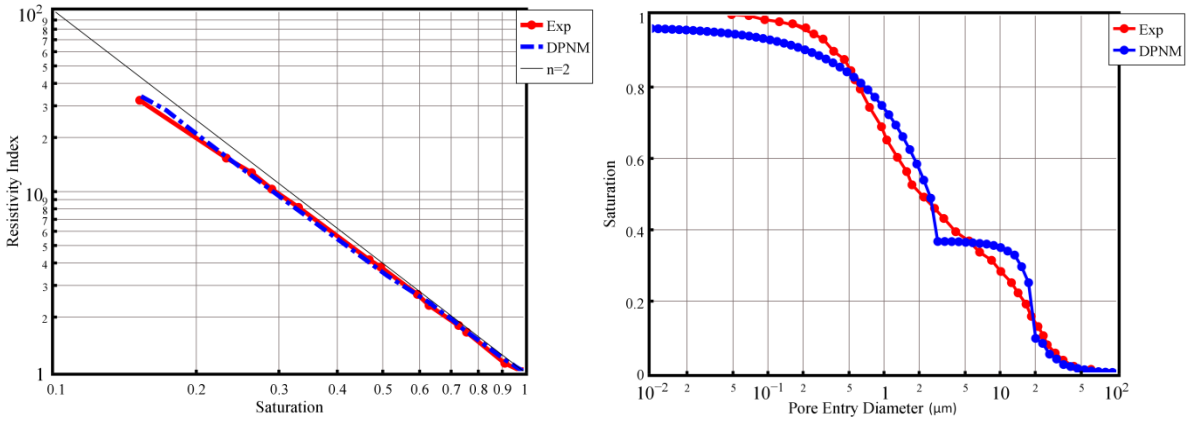

Figure 5. Lavoux carbonate sample: (left) resistivity index vs. saturation, (right) pore entry diameter distribution

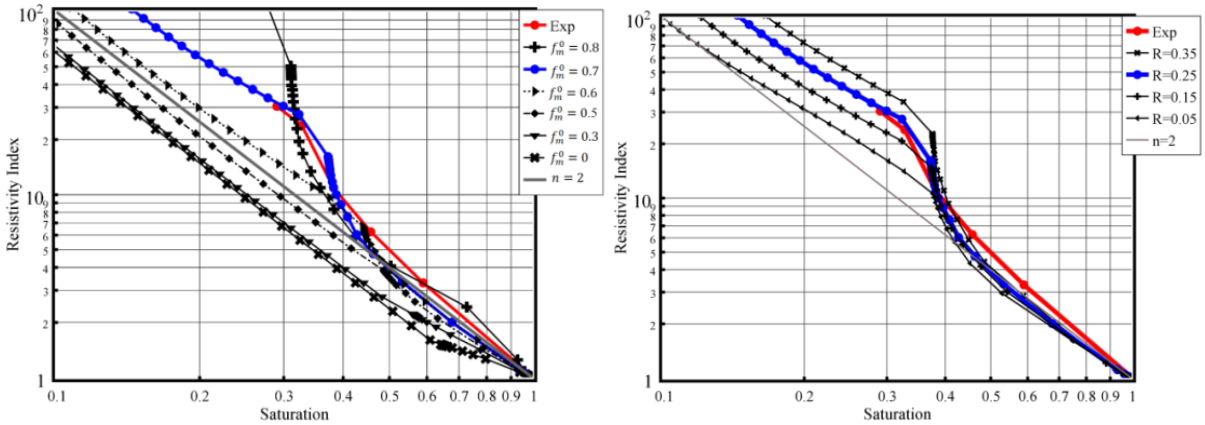

(a) (b)

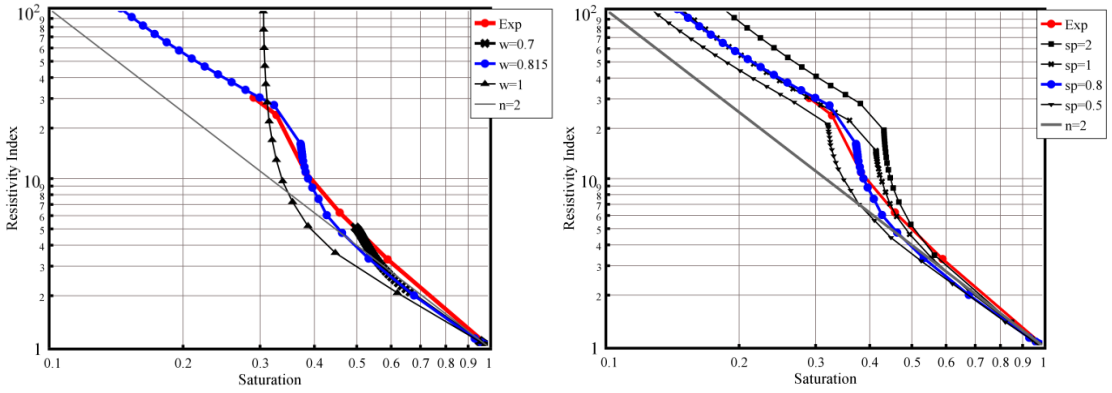

(c) (d)

Figure 6. Electrical response of Estaillades carbonate sample: (a) effect of zero matrix porosity fractions; (b) effect of size ratio R; (c) effect of connectivity exponent ω; (d) effect of the shape of vug size distribution.

REFERENCES

1. Focke, J. W., Munn, D., "Cementation Exponents in Middle Eastern Carbonate Reservoirs", *Soc. Petr. Eng*. 13735, (1985), 155-167.
2. Fleury, M., Y., "Resistivity in Carbonates: New Insights", *Proceedings of the Annual Symposium of the Society of Core Analysts*, (2002), Monterey, USA.
3. Dixon, J. R., Marek, B. F., "The Effect of Bimodal Pore Size Distribution on Electrical Properties of Some Middle Eastern Limestone", *Soc. Petr. Eng*. 20601, (1990), 743-750.
4. Petricola, M.J.C., Watfa, M., "Effect of Microporosity in Carbonates: Introduction of a Versatile Saturation Equation", *Soc. Petr. Eng*. 29841, (1995), 607-615.
5. Sen, P.N., "Resistivity of Partially Saturated Carbonate Rocks with Microporosity", *Geophysics*, (1997) 62, 2, 415-425.
6. Han, M., Tariel, V., Youssef, S., Rosenberg, E., Fleury, M., Levitz, P., "The Effect of the Porous Structure on Resistivity Index Curves. An Experimental and Numerical Study", *SPWLA 49th Annual Logging Symposium*, (2008), 1-10.
7. Bauer, D., Youssef, S., Fleury, M., Bekri, S., Rosenberg, E., Vizika, O., "Improving the Estimations of Petrophysical Transport Behavior of Carbonate Rocks Using a Dual Pore Network Approach Combined with Computed Microtomography", *Transp. Porous. Med.*, (2012) 94, 505-524.
8. Ioannidis, M. A., Chatzis, I., "A Dual-Network Model of Pore Structure for Vuggy Carbonates", *Proceedings of the Annual Symposium of the Society of Core Analysts*, (2000), Abu-Dhabi, U.A.E.
9. Ioannidis, M. A., Chatzis, I., "Network Modeling of Pore Structure and Transport Properties of Porous Media", *Chemical Engineering Science*, (1993) 8(5), 951-972.
10. King, P. R., "The Use of Renormalization for Calculating Effective Permeability", *Transport in Porous Media*, (1989)4, 37-58.
11. Nakashima, Y., Nakano, T., "Accuracy of formation factors for three-dimensional pore-scale images of geo-materials estimated by renormalization technique", *Journal of Applied Geophysics*, (2011) 75, 31–41.